

UNIVERSITY OF TARTU
FACULTY OF MATHEMATICS AND COMPUTER SCIENCE
Institute of Computer Science
Computer Science

Kristjan-Julius Laak

Investigating the phase transition in human brain at the moment of awakening

Bachelor's thesis (6 ECTS)

Supervisors: **Raul Vicente**

Jaan Aru

Seminar supervisor: Margus Niitsoo

Tartu 2014

Investigating the phase transition in human brain at the moment of awakening

Abstract:

We take granted the ability to fall asleep or snap out of sleep into wakefulness, yet these transitions change our mental state completely and sometimes (e.g. fire alarm) very quickly. In this interdisciplinary study, modern computational techniques were applied to a relatively unique set of human brain data recorded from the scalp while the subjects were repeatedly woken up from asleep. A novel algorithm was built to automate the phase of cleaning the recordings from non-brain-related signals. With the aim to characterize the transition from sleep to wake state, many quantitative approaches were used and a state space technique was developed to examine these brain recordings. The awakening was associated with slow cortical potentials, an increase in power of a broad range of frequencies, emergence of gamma power, and a transpose in the state space.

Key words: Electroencephalography, transition, sleep, state mapping

Faasimuutuse uurimine inimaju ärkamismomendil

Lühikokkuvõte:

Küsimus selle kohta, mis toimub meie aju sel hetkel, kui ärkame üles uneseisundist, puudutab meid kõiki. Käesolevas interdistsiplinaarses töös kasutati kaasaegseid arvutuslikke meetodeid uurimaks aju elektrilist aktiivsust üleminekul unefaasist ärkvelolekusse. Töö raames arendati välja uudne algoritm eemaldamaks ajuandmetest mitte ajuga seotud signaale. Ärkamismomendi kirjeldamiseks kasutati nii mitmeid üldtuntud kvantitatiivseid meetodeid kui ka inimaju elektriliste signaalide kujutust dünaamilisse olekute ruumi. Ärkamishetkega seostati aeglaseid ajupotentsiaale, üle kõikide ajusageduste ilmnevat võimsuse tõusu, gamma sagedusriba jõudluse esilekerkimist ja ajusignaalide karakteristikute olulist asukoha muutust olekute ruumis.

Võtmesõnad:

Elektroentsefalograafia, faasimuutus, uni

Contents

Introduction	4
1. Biological background.....	6
2. Methods.....	8
2.1. Sleep experiment data	8
2.2. Pre-processing.....	9
2.3. Analysis of the data	14
3. Results.....	19
3.1. Pre-processing.....	19
3.2. Event-related potentials	19
3.3. Fourier analysis	23
3.4. Time-frequency representation.....	25
3.5. State space analysis	28
4. Discussion	30
4.1. Main results.....	30
4.2. Methodological considerations	32
4.3. Future work	33
Conclusions	34
References	35
Appendix	38
I MATLAB code.....	38
II Licence.....	39

Introduction

Waking up is such a common experience – each of us has done it thousands of times – yet it is also mysterious, because the mental state changes completely and sometimes very quickly. Although many studies have described the mental state changes before, the more complex and dynamic processes of the phase transitions in humans have been poorly investigated [1]. The principles that govern these brain state switches could be used to build applications that could detect sleep-wake transitions simply by the bioelectrical activity of the brain. Every year hundreds of thousands of car accidents are caused by the driver’s inability to monitor his or her alertness state [2]. Applications that could prevent accidents caused by drivers who fall asleep behind the wheel could save many lives e.g. when used to stop the vehicle when the driver becomes too drowsy. *Vice versa*, when we know the characteristics of the sleep-wake transitions, it would be possible to initiate these transitions in the brain by electro-magnetic stimulations or drug administration. In any case, understanding the sleep-wake transitions may ultimately have broad implications in many areas of science, medicine, and everyday life [3].

Because of the vast amount and complexity of the data collected from the brain recordings, explicit quantitative results can in general be obtained only through numerical and computational methods [4]. Recent advances in computational neuroscience (CNS) – the interdisciplinary field between computer science and neuroscience – has led to many mathematical models providing a natural explanation for the sleep-wake transitions (e.g. [4]–[7]). Although these models explain how and why state changes occur, they fail to provide any quantifiable variables representing the onset of consciousness transition in humans [8]. In this thesis, mathematical and computational tools are applied to a relatively unique set of human brain data recorded while the subjects were repeatedly woken up from asleep. These data are relatively unique in the sense that not many laboratories in the world have human EEG recordings of the moment of awakening. The purpose of this thesis is to characterize the electrophysiological transition from sleep to wakefulness in humans.

In Chapter 1, a concise overview of the anatomy of the brain, electrical brain rhythms, and mental state transitions is given. In Chapter 2, the methodological part of the study is presented. All the analysis of brain signals recorded from the scalp start with the most tedious part of any biological signal analysis – cleaning the recordings from non-brain-related activity. In the first stage of this study, a novel algorithm was developed to automate some aspects of this pre-processing phase. In the second stage, modern computational methods were used to characterize

the sleep-wake transition. First, the bioelectrical potentials characterizing this phase transition were investigated in the time domain. Then the transformation of the frequency domain was explored. Next, the time-frequency representation of the transition was computed to explore how the transition evolves over time. Last, to determine the dynamics between the sleep and wakefulness, the recordings were analyzed with a multidimensional state-mapping technique. The previous studies have used state space analysis on data recorded in mice and rats (e.g. [9]), but in this study, the technique was adjusted to examine the dynamics of the sleep-wake transition in humans. In Chapter 3, the results of this study are visualized and presented in detail. The Chapter 4 discusses the results with respect to the other studies and the aims of this thesis. In Appendix, the scripts written for processing and analysis are provided (on-line) and the license for online publishing is included.

1. Biological background

The outer part of the human brain is called cerebral cortex and can broadly be divided into four lobes: frontal, parietal, occipital and temporal lobes [10]. The inner part of the cerebral cortex is the white matter, which is composed of bundles of nerve fibres. The outer part covering the neuronal fibres is greyish structure, which contains mainly the cell bodies of the neurons. The nerve cells produce electrical potentials and large groups of neurons in the cerebral cortex produce electrical potentials large enough to be measured by electrodes placed on the scalp [11]. The method of recording electrophysiological brain activity from the scalp (i.e. non-invasively) is known as electroencephalogram (EEG).

The electrical signals of the brain are mostly rhythmic and can be subdivided into frequency bands historically named after the letters of the Greek alphabet: δ (0.5-3 Hz), θ (4-7 Hz), α (8-15 Hz), β (16-29 Hz), and γ (30-100+ Hz). Brain waves are used to distinguish between different mental states, e.g. the relaxed wake state can be characterized by low-amplitude α oscillations, whereas by the transition to light sleep higher amplitude θ waves emerge and mix with α -rhythms [12].

When we fall asleep, increasingly prominent slow waves (0.5-7 Hz) gradually emerge. This phase of sleep is called slow-wave sleep (SWS) or non-rapid eye movement (NREM) sleep, as opposed to another phase of sleep named rapid eye movement (REM) sleep. The transition from wakefulness (W) to SWS or vice versa involves dramatic behavioural changes – e.g. breathing, heart rate, and eye closure – that are not instantaneous and could take several minutes in humans. Yet, as we monitor EEG from the scalp, we see that the actual electrophysiological transition in the human brain occurs over just a few seconds [13].

One proposed model explains the abrupt changes happening during sleep-wake transitions as are seen in electronic flip-flop switches [3]. This switch is implemented in the mouse brain by a competition between two distinct mutually inhibitory groups of neurons. Although these neurons lay deep in the brain in a region called brainstem, they are incorporated into brain's electrical circuits and ensure a rapid and complete state transition. The two neuronal populations regulating the sleep-wake switch consist of either sleep-promoting (SWS-specific) or waking-promoting (W-specific) neurons [13]. Most importantly, at the transition from SWS to W (in response to a sudden stimuli e.g. arousing sound) the W-specific neurons deep in the brain begin to fire as early as 1.0 seconds prior to the onset of EEG activation on the outer part of the brain [9]. As the human brainstem is organized very similarly to the brainstem of mice, in this thesis we

hypothesize that the transition between the N1 sleep and W state seen in EEG activation takes about 1 second also in humans.

2. Methods

2.1. Sleep experiment data

2.1.1. Subjects and awakening procedure

The sleep experiments were conducted by the author in the Laboratory of Cognitive Neuroscience in Tallinn. Four healthy subjects participated in the sleep experiments where they were repeatedly awoken from the sleep onset period. The latter sleep stage is also known as NREM stage 1 (or in short N1). To mask the environmental noise, a continuous pink noise audio file was played through in-ear headphones (Yamaha Corporation). The subjects were woken up by stopping the auditory stimulation and calling their name at the same time (in short, awakening stimulus). Importantly, the time of awakening was marked manually and thus the exact moment of awakening has a precision of 0.5 seconds. When the subjects had been awake for a few minutes, they were instructed to fall asleep again. The procedure was repeated until around 40 awakenings were obtained from each subject. All the participants read and signed written informed consent form and they were paid for participation. Sleep experiments have been approved by the Ethics Review Committee on Human Research of the University of Tartu.

2.1.2. EEG recordings

EEG was recorded by Nextim eXimia EEG-system with 60-carbon electrodes cap (Nexstim Ltd., Helsinki, Finland) to manually score sleep stages. In every recording, all 60 electrodes were used (FP1, FPZ, FP2, AF1, AFZ, AF2, F7, F5, F1, FZ, F2, F6, F8, FT9, FT7, FC5, FC3, FC1, FCZ, FC2, FC4, FC6, FT8, FT10, T3, C5, C3, C1, CZ, C2, C4, C6, T4, TP9, TP7, CP5, CP3, CP1, CPZ, CP2, CP4, CP6, TP8, TP10, P9, P7, P3, P1, PZ, P2, P4, P8, P10, PO3, POZ, PO4, O1, OZ, O2, IZ). The reference electrode was placed on the forehead. All EEG signals were sampled at 1450 Hz sampling rate and processed with hardware based high-pass filter of 0.1 and low-pass filter of 350 Hz. All the data were visually inspected and trials referring to other stages than N1 (W or other stage of NREM) were excluded from the analysis. Note that throughout this thesis, the electrodes are interchangeably called also channels.

2.2. Pre-processing

2.2.1. MATLAB software

For all of the processing and analysis done in this thesis, MATLAB® (2013a) software (MathWorks, Natick, MA, U.S.A.) was used. Besides being a high-level language for computation, visualization, and programming [14], MATLAB is the foundation solution of many toolboxes for mathematics, statistics, signal processing and even computer vision. Some of the scripts written for the thesis use a MATLAB software toolbox FieldTrip [15]. FieldTrip is an open source toolbox for EEG analysis, developed at the Donders Institute for Brain, Cognition and Behaviour at the Radboud University Nijmegen, the Netherlands, and published under the GNU general public license [16].

2.2.2. Preparation of the data

The data from the sleep experiment was recorded only some time before and after the awakening. Thus, the different recordings (trials) had to be appended to each other to form a compound dataset. The first part of this study was pre-processing of the raw data, i.e. removing noise and signal that was not of interest (i.e. artifacts), for which a novel MATLAB algorithm was developed by the author.

Prior to concatenating, the trials were processed with FieldTrip function `ft_preprocessing`. The latter function reads EEG data and applies several pre-processing steps to the signal specified in a configuration structure [17]. The configuration structure contains all the information about the dataset, trials, and pre-processing options (e.g. the trial definition). The trials were defined by a custom function, assigning a 3 seconds pre- and post-awakening time point to each trial, based on a previously formed vector of moments of awakenings. During the pre-processing, the raw continuous data of each trial was digitally filtered with a low-pass filter of 90 Hz, with a padding of 1.5 seconds, and demeaned with a baseline window of -100 to 0 ms as measured with regard to the awakening stimulus. With the low-pass filter, all the frequencies higher than 90 Hz were eliminated from the data, resulting in less noisy and smoother signal. The function `ft_preprocessing` returns a FieldTrip specific data structure, containing the individual trials, channel names and time vectors for each of trial.

For each subject, a FieldTrip function `ft_appenddata` was used to append all the preprocessed trials collected from one experiment night into a single Fieldtrip data structure [18]. The output structure of `ft_appenddata` is the same as of the function `ft_preprocessing`.

2.2.3. Artifacts in the EEG recordings

Most of the biological signals, such as EEG, appear as weak signals combined with many other signals of various origins [19]. For example, the 50 Hz power supply waveform (the line-noise) is apparent in most of the instrumentation used in EEG recordings. EEG is also sensitive to any head movement, muscle contraction, and even eye movement, posing an interference or artifact to the signal. In order to clean the datasets from such artifacts, a custom method was developed in MATLAB.

2.2.4. An algorithm for detecting invalid channels

In a regular artifact rejection protocol, epochs of EEG data or the channels contaminated with artifacts are thrown out. Due to the aims of the thesis and the nature of the sleep experiment, simply rejecting contaminated epochs results in a considerable loss of collected information. The best approach with the kind of sleep EEG data was to identify all the bad channels (i.e. channels with too high amplitude, artifacts or low validity), and try to interpolate them with the nearest channels that are not contaminated.

The bad channel detection was performed on the pre-awakening period of the data, as brain activity of a sleeping subject contains less artifacts than the activity of an awake subject. In order to detect the bad channels, the following algorithm was used for each trial.

First, channels with absolute amplitudes over 250 μV were marked as contaminated. The amplitude estimation was based on the fact that the intrinsic amplitude of EEG signal measured from the scalp for a typical adult human is about 10 μV to 100 μV [20].

Second, each channel was standardized to a unit variance with the formula

$$X_s = \frac{X - \mu}{\sigma}$$

where X_s is the standardized channel vector, X the original channel vector, μ is the median of the channel, and σ the standard deviation of the channel.

Third, for each standardized channel, the Euclidean distance from the median of the normalized trial matrix was calculated. This resulted in a number describing the overall distance of the channel from the median of the whole trial matrix.

Fourth, for each trial, a probability density estimate of the samples in the channel norms vector was computed with the MATLAB function `ksdensity` (Figure 1A). The function `ksdensity` evaluates the density estimate at 100 points covering the range of the data in the input vector.

The estimate is based on a normal kernel function, using a window parameter (bandwidth) that is a function of the number of points in the input vector [21].

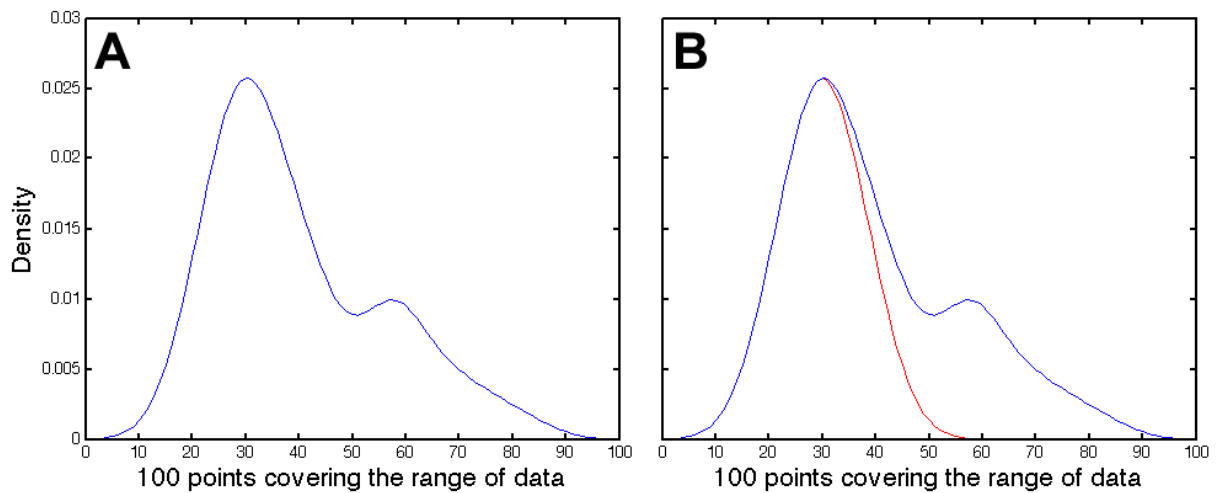


Figure 1. **A.** Probability density estimate plots for each channel per trial. **B.** The red line on is a reflection of the left side curve from the maximum point, simulating a Gauss curve.

It was intuitively presumed that the Euclidean distances of the clean channels' norms follow a Gauss curve, i.e. the distances of the clean channels from the median follow a normal distribution. Alternatively, it was presumed the distance from median of bad channels deviate from the Gauss distribution of the clean channels. This was based on the fact that the data was collected carefully with respect to electrodes' impedance.

Fifth, to simulate a Gauss curve, the maximum of the density estimate was found, and the curve from the left side of the maximum was mirrored to the right side of the maximum. To determine the contaminated channels by the density estimate plot seen above, the channels farther than the end of the mirrored curve were marked as contaminated (Figure 1B).

Unfortunately, for most of the trials recorded in the end of a long recording night, not many channels remained clean. For these trials, the density estimate curve had too many trials "in" the curve presumed to describe the distribution of clean channels.

Thus, for these trials, the "cut off" point was marked at the third quartile of the Gauss curve. This was a compromise between marking too many clean channels as bad and still marking some of the channels as invalid. After the procedure, some channels were marked as invalid. The head model for electrode positions and red electrodes indicating a possible resultant bad channels detected by the algorithm is illustrated in the Figure 2.

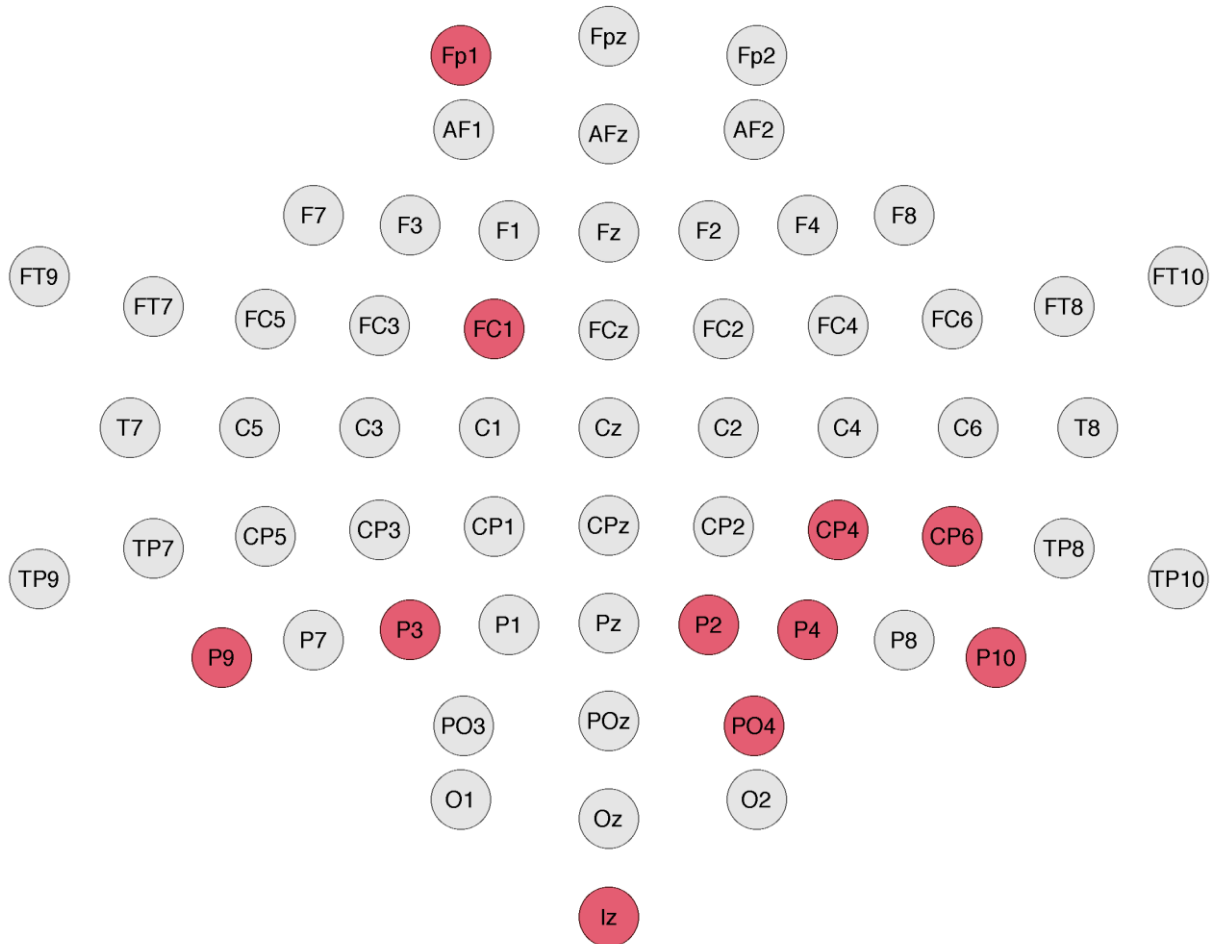


Figure 2. Head model with all the electrodes (channels) with red circles indicating bad electrodes detected by the algorithm using probability density estimation.

2.2.5. Interpolating

The interpolation of previously marked channels was done using FieldTrip function `ft_channelrepair`. The function uses nearest-neighbour approach to repair bad channels in EEG data by replacing the activity of these channels with the average of their neighbours weighted by distance [22]. The method uses a neighbourhood structure, i.e. predefined structure defining the neighbouring channels for each channel. Unfortunately, the nearest-neighbour approach cannot be used reliably to repair multiple bad channels that lie next to each other. Thus, the neighbourhood structure had to be modified for each trial separately so that no channel that needed to be repaired had neighbours that needed to be repaired themselves. If a channel had less than two neighbours after altering the latter structure, the channel was not interpolated. After interpolating, the final decision of which channel to keep in the dataset was done visually. It is

important to notice that per one dataset with all the trials recorded from one experiment night of one subject, a bad channel in one trial meant removing the channel from all of the trials. Thus, trials with an excessive amount of bad channels compared to the other trials were outright rejected from the dataset.

2.2.6. Visual rejection

The final decision of which channels to keep was done visually using FieldTrip function `ft_rejectvisual`. The function guides the user through all the data to visually select the trials that should be rejected, i.e. thrown out of the dataset [23]. This manual approach was chosen after a thorough study of the data and automatic data rejection methods available. Visual inspection was chosen also because there was a possibility that some of the channels that were not interpolated were eventually clean channels and vice versa, and removing too many or not enough channels per dataset would result in poor data.

2.2.7. Independent component analysis

If during an EEG acquisition procedure the subject moves eyes suddenly, the signal will be distorted heavily. A common way for removing eye movement artifacts from EEG data is to use independent component analysis (ICA).

ICA is an elegant and practical computational blind source separation method to recover a set of underlying components which are statistically maximally independent from each other [24]. The resultant components are automatically sorted based upon on the sum of the weighting factors. Determination of the components with eye movement artifacts was aided by spatial topography of the components. An illustration of the components can be found in Figure 3.

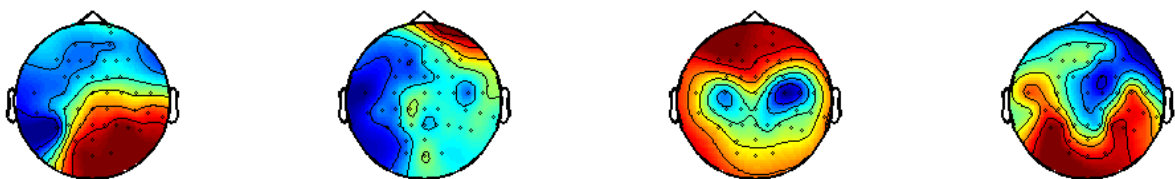


Figure 3. The spatial topography of the ICA components were used to determine the eye movement artifacts. In this illustration, the second head model from the left represents such artifact.

A trained eye can relatively easily spot the components that represent artifacts from the eye movements [25]. After performing ICA, the components identified as eye movement artifacts

were rejected and the data back-projected to its original form. Last, the 50 Hz line-noise was removed by applying a notch filter to the data using Fieldtrip function `ft_preproc_dftfilter` [17]. The difference between the raw and pre-processed data is illustrated in the Figure 4 below.

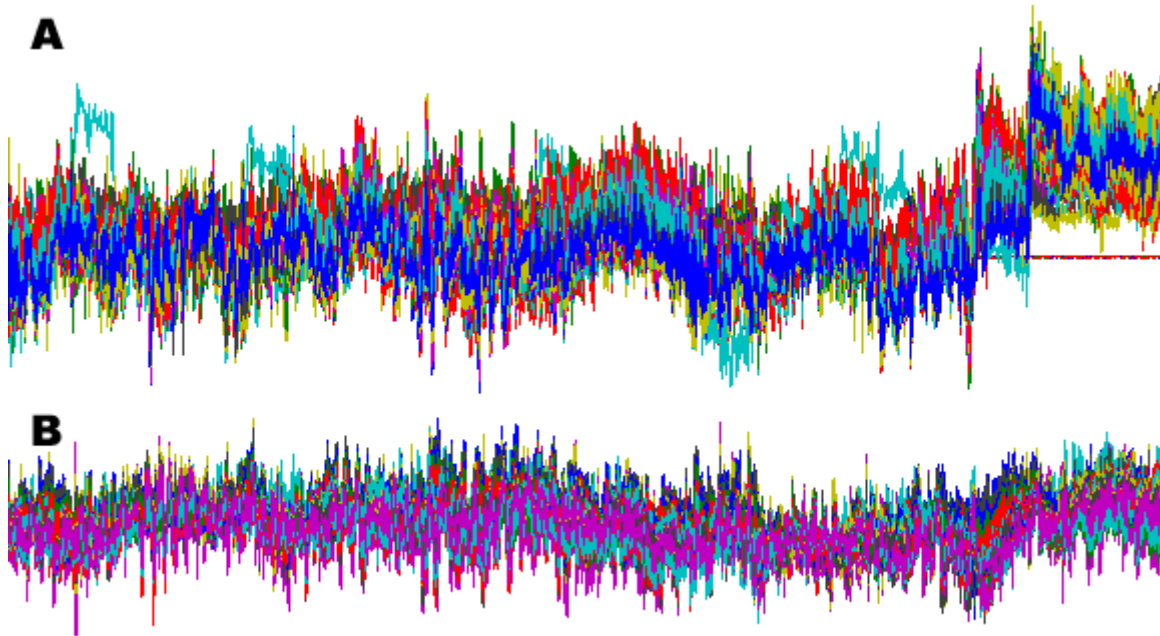


Figure 4. The difference between raw data **(A)** and pre-processed data **(B)** for the same trial. Different colours mark different channels.

2.3. Analysis of the data

2.3.1. Regions-of-interest

After the visual inspection, some channels were rejected from the dataset. This was done for each dataset representing trials recorded from one night. For the following analysis, it was reasonable to concatenate the data sets of one subject recorded at different experiment nights. As the rejected channels differed from dataset to dataset, the 60 channels were divided into regions-of-interest (ROI). This allowed to look at ROIs instead of individual channels and thus eliminate the differences in channels between datasets. The channels were grouped into seven ROIs by the spatial topography and well known anatomical separation of brain areas [10]:

- 1) Centro-frontal (CF) region for electrodes Fp1, Fpz, Fp2, AF1, AFz, AF2, F1, Fz, F2;
- 2) Left anterior (LA) region for electrodes F7, F3, FT9, FT7, FC5, FC3, T7, C5, C3;
- 3) Centro-medial (CM) region for electrodes FC1, FCz, FC2, C1, Cz, C2, CP1, CPz, CP2;

- 4) Right anterior (RA) region for electrodes F4 , F8, FC4, FC6, FT8, FT10, C4, C6, T8 ;
- 5) Left posterior (LP) region for electrodes TP9, TP7, CP5, CP3, P9, P7, P3;
- 6) Centro-occipital (CO) region for electrodes P1, Pz, P2, PO3, POz, PO4, O1, Oz, O2, Iz;
- 7) Right posterior (RP) region for electrodes CP4, CP6, TP8, TP10, P4, P8, P10 (Figure 5).

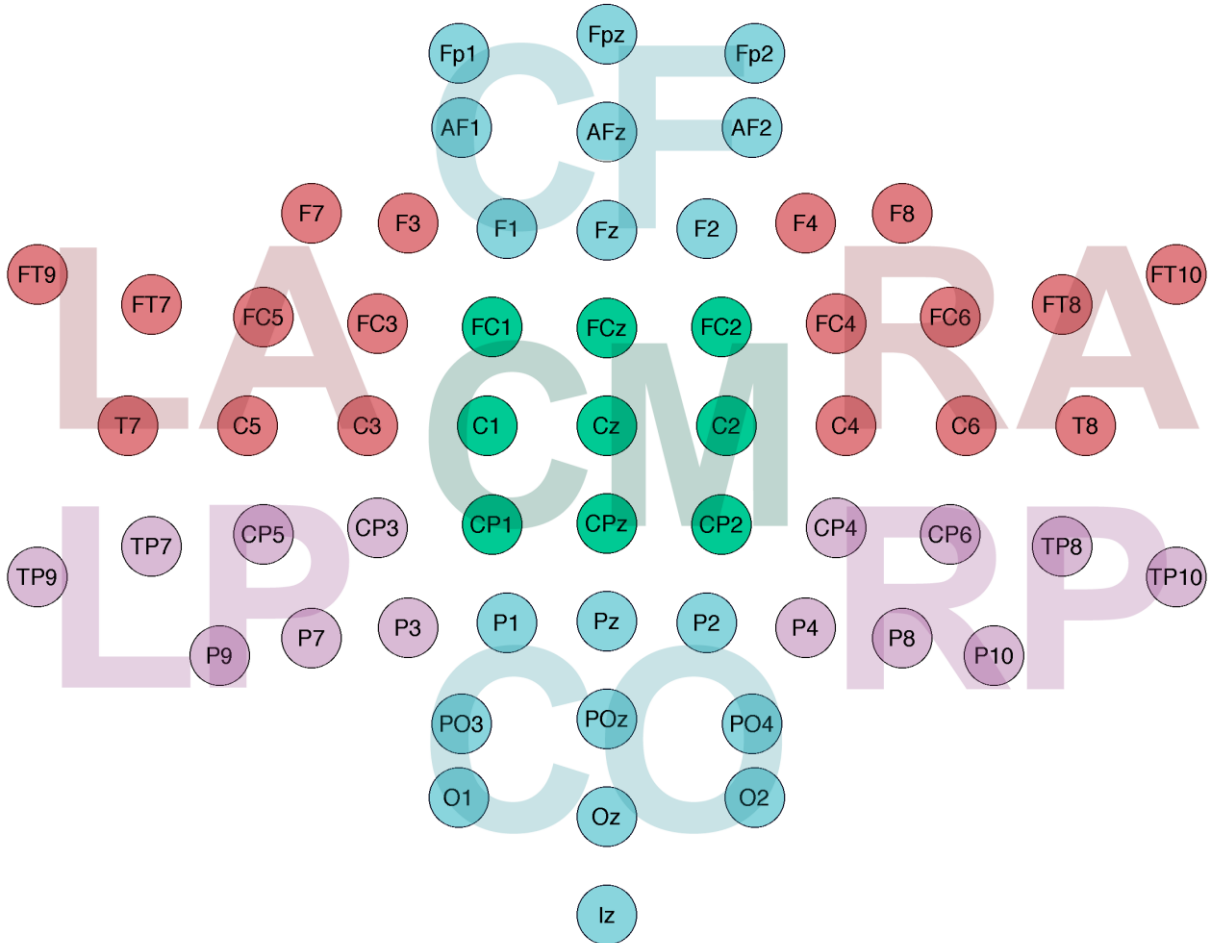


Figure 5. The topographic representation of the electrode positions and the seven regions-of-interest illustrated in colour and transparent abbreviations.

Grouping the channels per trial was done by averaging the set of channels into a single time series. For each subject of the three whose data was recorded during more than one night, the datasets containing ROIs were appended to each other.

2.3.2. Event-related potentials

The brain activity measured by EEG that could be seen in response to an external stimuli (e.g. flashlight, fire alarm) is called event-related potentials (ERP). In general, ERPs are weak signals buried in noise and ambient background activity of associated neural systems [19]. Thus, by

looking at the data of a single trial it is hard to detect by eye the waveforms characterizing an awakening. One way of increasing signal-to-noise ratio (SNR) is to use (synchronized) averaging of the data across the trials and see if ERPs are seen more clearly (Due to the sleep experiment conditions, the data of this thesis has an awakening stimulus with an precision of 0.5 s, and the word *synchronized* is used in parenthesis). Another advantages of (synchronized) averaging is that it is faster than most frequency-domain filtering, requiring no spectral characterization of the signal and noise [19].

Since the amplitude and characteristics of the EEG signal vary across the subjects, experiments, and even trials, the data was normalized by rescaling the trials to a range of [0, 1]. The equation of the normalization is given as

$$X_{norm} = \frac{X - \min(X)}{\max(X) - \min(X)}$$

where X is the original trial data obtained from pre-processing and X_{norm} is the normalized trial. Each averaged signal was also applied a baseline correction (divided by mean) of -200 to 0 ms before awakening stimulus. The averaged signal vector of was further smoothed using a moving average filter with a window of 0.1 second.

2.3.3. Discrete Fourier transform

The basic discrete events in time, such as ERPs and variance can indeed be assessed in the time domain. However, the latter representation of waveforms has several disadvantages, such as the signal differs from trial to trial, and it does not convey frequency-domain characteristics. In the other hand, most of the brain states in wake-sleep cycle can be characterized by the different waveforms present in EEG.

One way to compute frequency representation of a signal is the Discrete Fourier transform (DFT). The DFT is commonly implemented with Fast Fourier transform (FFT) algorithm which is the most optimal way to compute DFT of a set of data x_0, \dots, x_{N-1} of length N . The formula of FFT is given as

$$X_f = \sum_{t=0}^{N-1} x_t e^{-i2\pi k \frac{t}{N}}$$

where f is the frequency of interest, and X_f is the energy of frequency f in the signal [26]. The DFT was computed for two different conditions: 3 seconds before and 3 seconds after awakening. It was seen from the power spectrums (absolute value to the power of two of the

Fourier transform) that the 50 Hz line-noise had been so strong, that even when removed with the notch filter, the adjoining values used for replacing the 50 Hz waveform were still high enough to leave a peak in the power spectrum. Therefore, the values between 49 and 51 Hz were explicitly replaced by the mean of the power of those two frequencies. The manual notch filter was applied as the initial Fieldtrip notch filter used had a static width of the filter.

2.3.4. Time-frequency analysis

The DFT reveals a general difference between the sleep and wake state in the frequency domain, but it lacks the ability to characterize the transition in time. To analyse the signal over the whole frequency domain and also localize the power change in time, the time-frequency representation (TFR) of the data was computed. This was done using a sliding window Fourier transform and Morlet wavelets (also known as Gabor wavelets, see [27]). The width of the wavelets in number of cycles was increased linearly from 4 to 12 for frequencies 2 to 90, increasing the frequency resolution for higher frequency component at the expense of time resolution and vice versa [28]. The TFR of the data was computed for the whole length of the trials, but plotted 2.5 seconds before and after the awakening with a baseline normalization (each time-frequency point divided by the mean baseline power of the respective frequency) of -1000 to -400 ms. The power changes were captured relative to the baseline because we were interested in the sleep-wake transition not in which mental state there is more absolute spectral power.

2.3.5. State space analysis

To gain insight into the dynamics of the transition from N1 sleep to wake state, a multidimensional state-mapping technique based on two spectral ratios was adopted. First used on rats to characterize the dynamics of large-scale forebrain wake-sleep cycle [1], the state space technique has been used on mice to study the sleep/wake states, movement between states, and transition processes [9]. To compute a two-dimensional state space, two spectral amplitude ratios were calculated by dividing integrated ranges of frequencies. First, a spectrogram was computed using a 0.5 second sliding window Fourier transform applied to the whole length of trials with a 0.2 second step. The window size was chosen to allow for a minimal frequency resolution of 2 Hz. To calculate the two spectral ratios, trapezoidal numerical integrations were computed over selected frequency bands from the absolute value of the spectral components and then divided by each other. The ratios were the following:

$$\frac{2 - 30}{2 - 90} \text{ Hz}$$

for Ratio 1 and

$$\frac{2 - 10}{2 - 30} \text{ Hz}$$

for Ratio 2. These frequency bands were chosen after a thorough search for parameters that would separate the sleep state from the awake state most clearly. Note that this is not a statistically flawed circular analysis, as the main goal of this thesis was to assess the activity in the period which is between these two states, i.e. the final analysis is independent of this selection. To gain more symmetrical distribution of the ratios, the frequency range of the numerator was always included in the frequency range of the denominator [1]. The frequency ranges used in this thesis differ from the previous state space works with rats and mice. The Ratio 1 with frequencies 2-30 Hz was chosen to emphasize all the oscillatory components below γ -band (30-100+ Hz). The spectral range of 2-10 Hz in Ratio 2 includes all the slow wave components (δ , θ , and low α band) prevalent in NREM sleep. Last, for each subject and trial principal component analysis (PCA) was applied to both of the spectral ratios. With an aim to narrow down the 7 ROIs to a single characterization of the transition, the first component of the PCA, explaining most of the variance, was used as an overall ratio measure. Both of the resulting components of ratios were further smoothed with a 2nd order Savitzky-Golay filter. The latter filter increases the signal-to-noise ratio by fitting successive set of data points with a polynomial by the linear least squares method [29].

For each of the data points in both of the final ratio vectors representing a spectral amplitude ratio of 0.5 second time window, a total of 28 steps (-3 to 3 seconds around awakening with a step of 0.2 seconds) were separated into sleep (steps 1-14), wake (20-28), and transition (15-19) sub-sets. The transition interval was chosen as we had a clear hypothesis: the EEG activation takes roughly 1 s from the awakening stimuli.

2.3.6. Permutation test

To determine whether the means of the clusters were statistically different from each other, a permutation test (also called randomization test) with 10,000 random permutations of the ratios was used. The difference between clusters was defined by the Euclidean distance between the two means, and p-value of the distance of the real means was computed by finding the proportion of the number of values higher than the real distance of all of the 10,001 computed distances.

3. Results

3.1. Pre-processing

Four healthy subjects (S1, S2, S3, S4) participated in the sleep experiment, and a total number of 183 awakenings (38, 51, 42, 52 for each subject, respectively) were used in pre-processing. Bad channel detection further selected trials to exclude from the further analysis, resulting in total of 127 awakenings used in successive analysis (35, 39, 21, 32 awakenings per subject, respectively).

3.2. Event-related potentials

As the brain activity in general varies from subject to subject, the ERPs were computed separately for each subject across all trials (Figure 6).

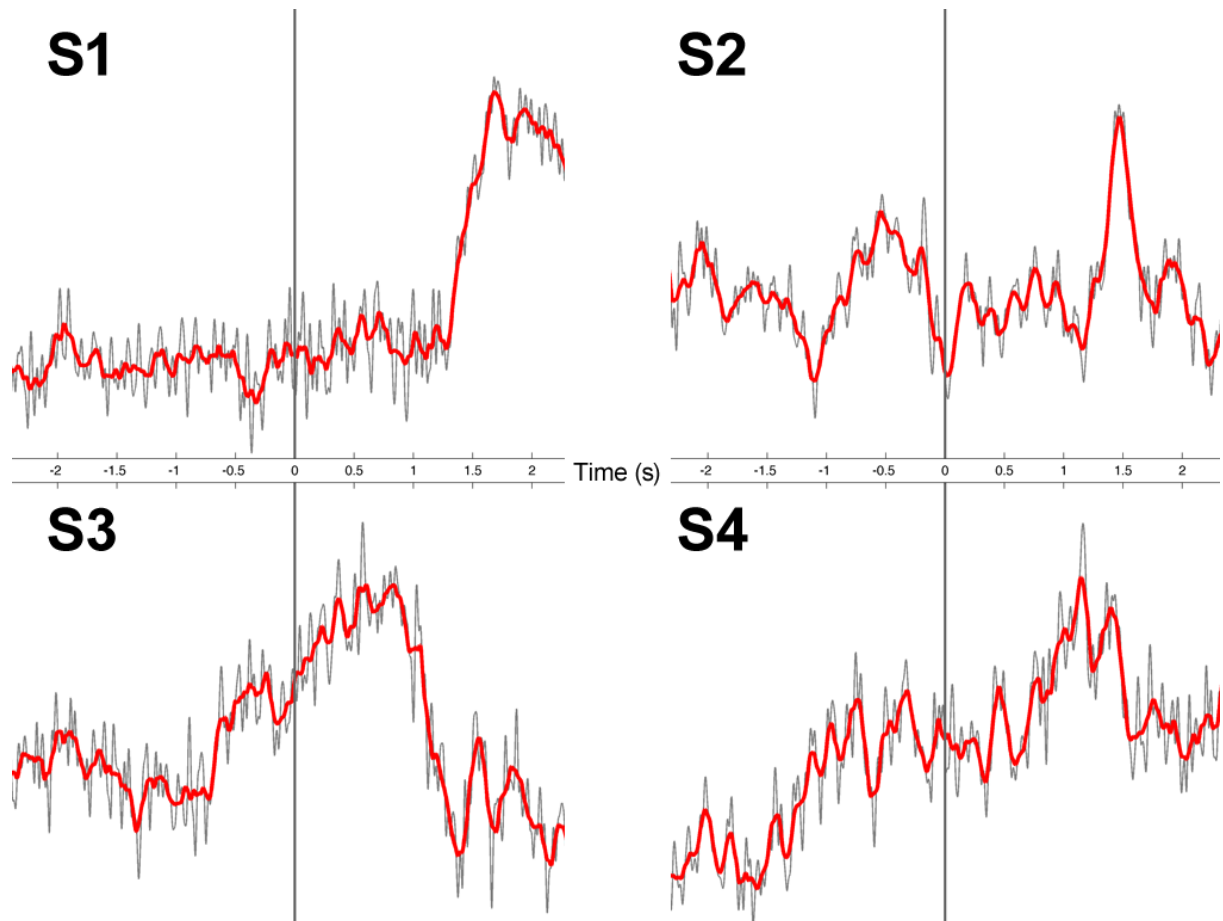


Figure 6. The ERPs were computed by averaging across trials for each subject (S1, S2, S3, S4). The smoothed signal is illustrated in red.

We can observe an amplitude shift from about 1 second after the awakening stimulus and it is clear that the brain response to awakening was different for the subjects. To further explore the difference within ROIs, the ERPs were computed in the single ROI-level for each subject. This topographic representation of the ROIs for each subject is illustrated on Figures 7, 8, 9, and 10 below.

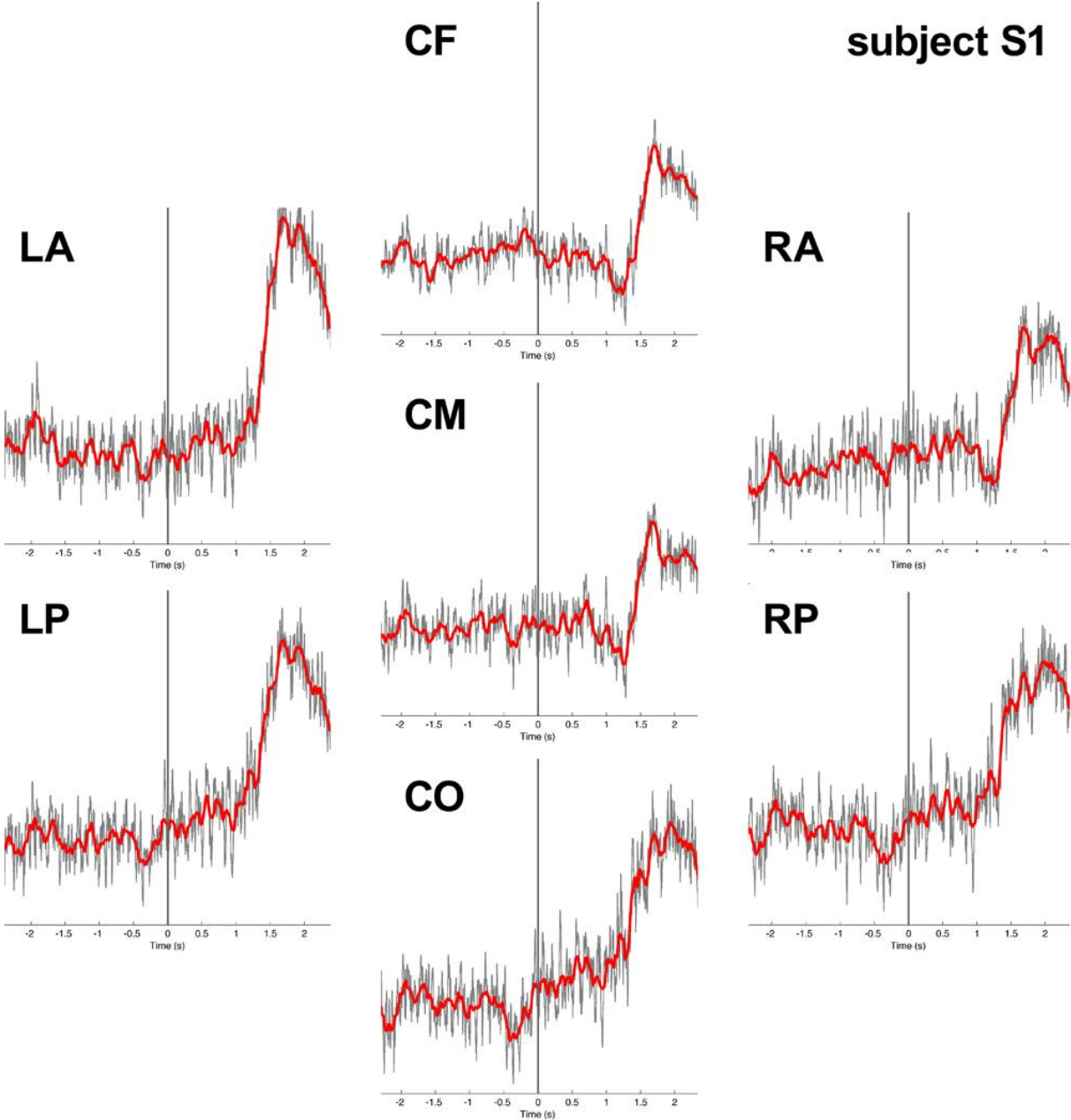


Figure 7. ERP plots for each ROI of subject S1, averaged across trials.

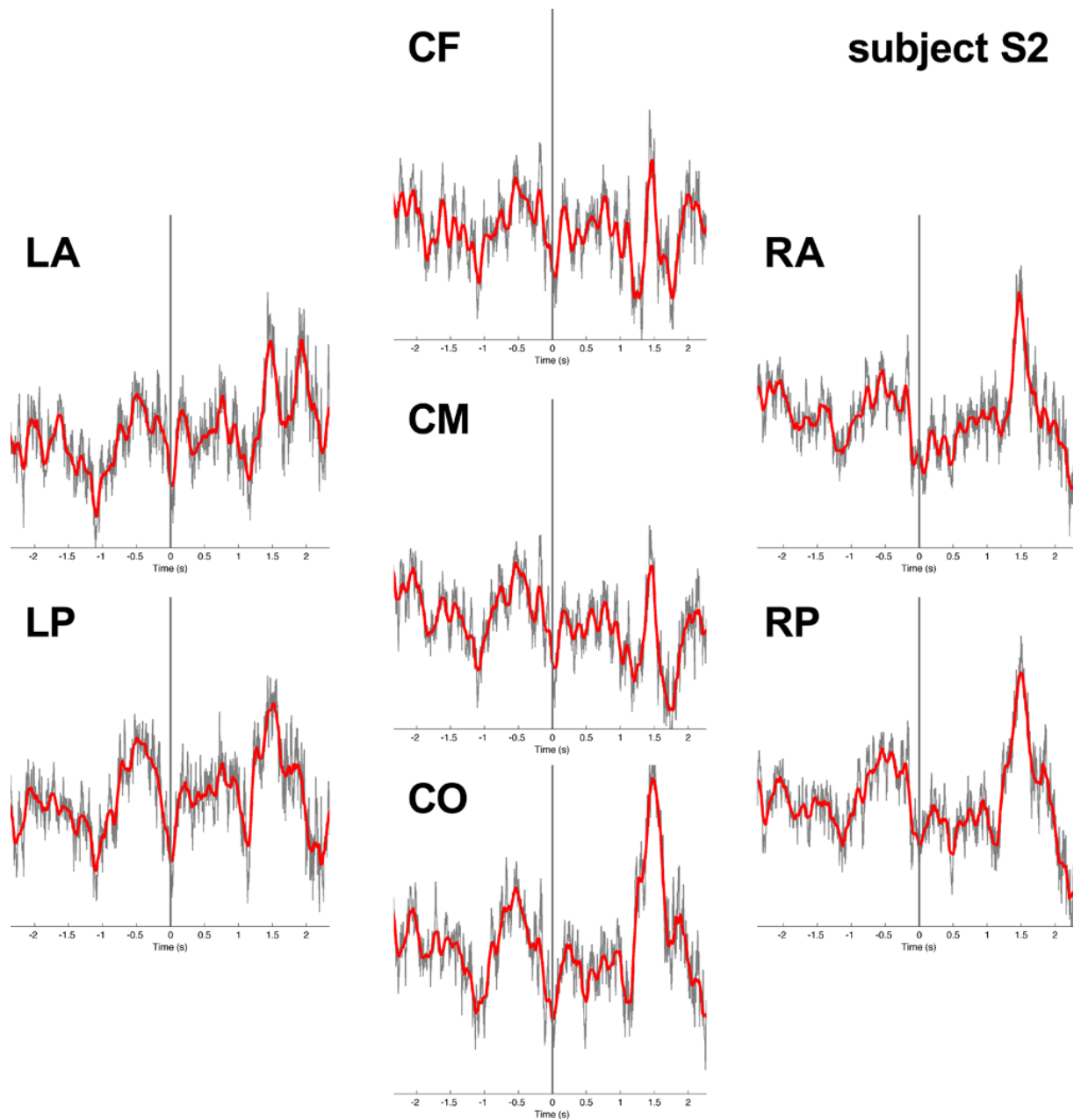


Figure 8. ERP plots for each ROI of subject S2, averaged across trials.

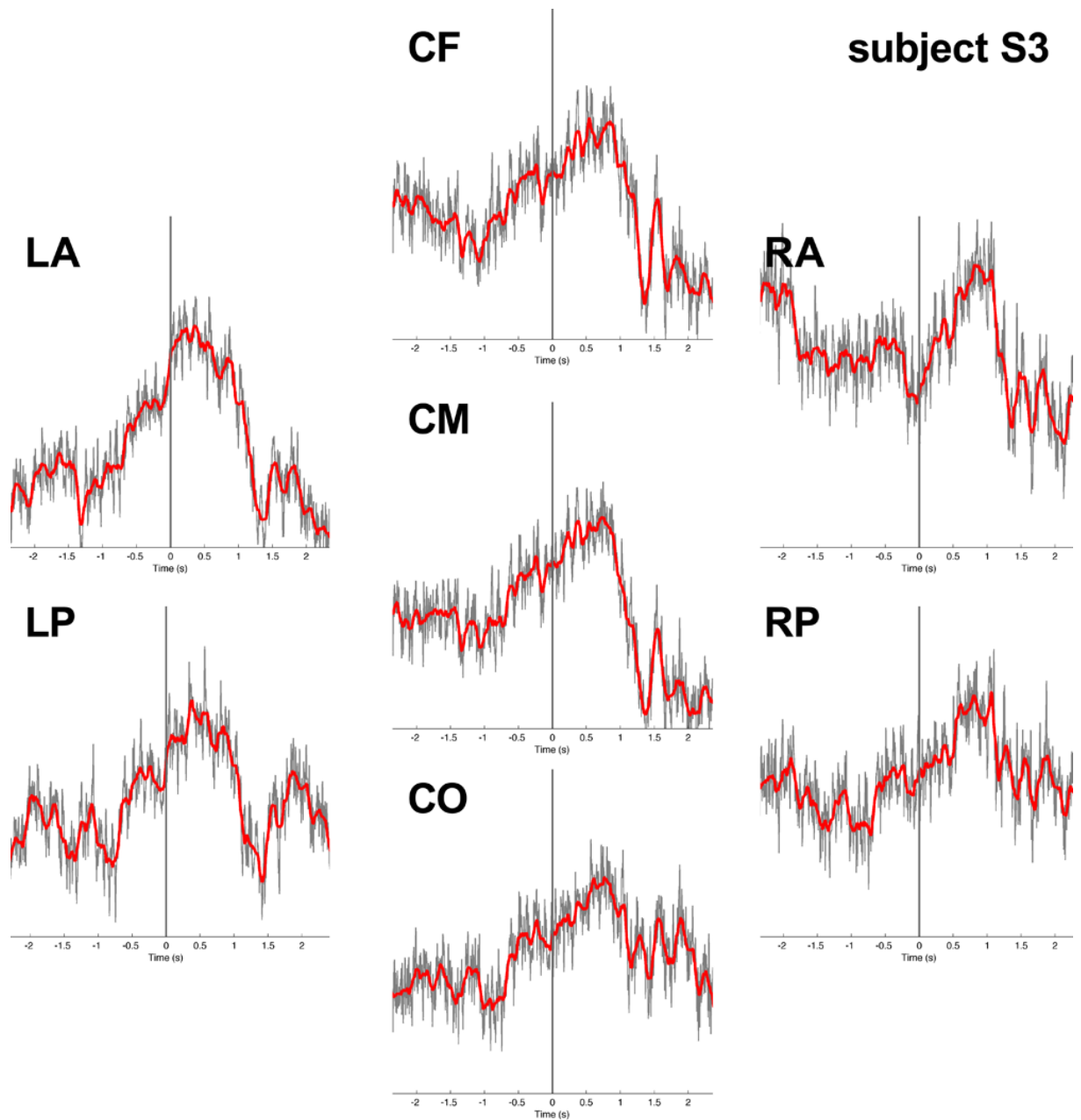


Figure 9. ERP plots for each ROI of subject S3, averaged across trials.

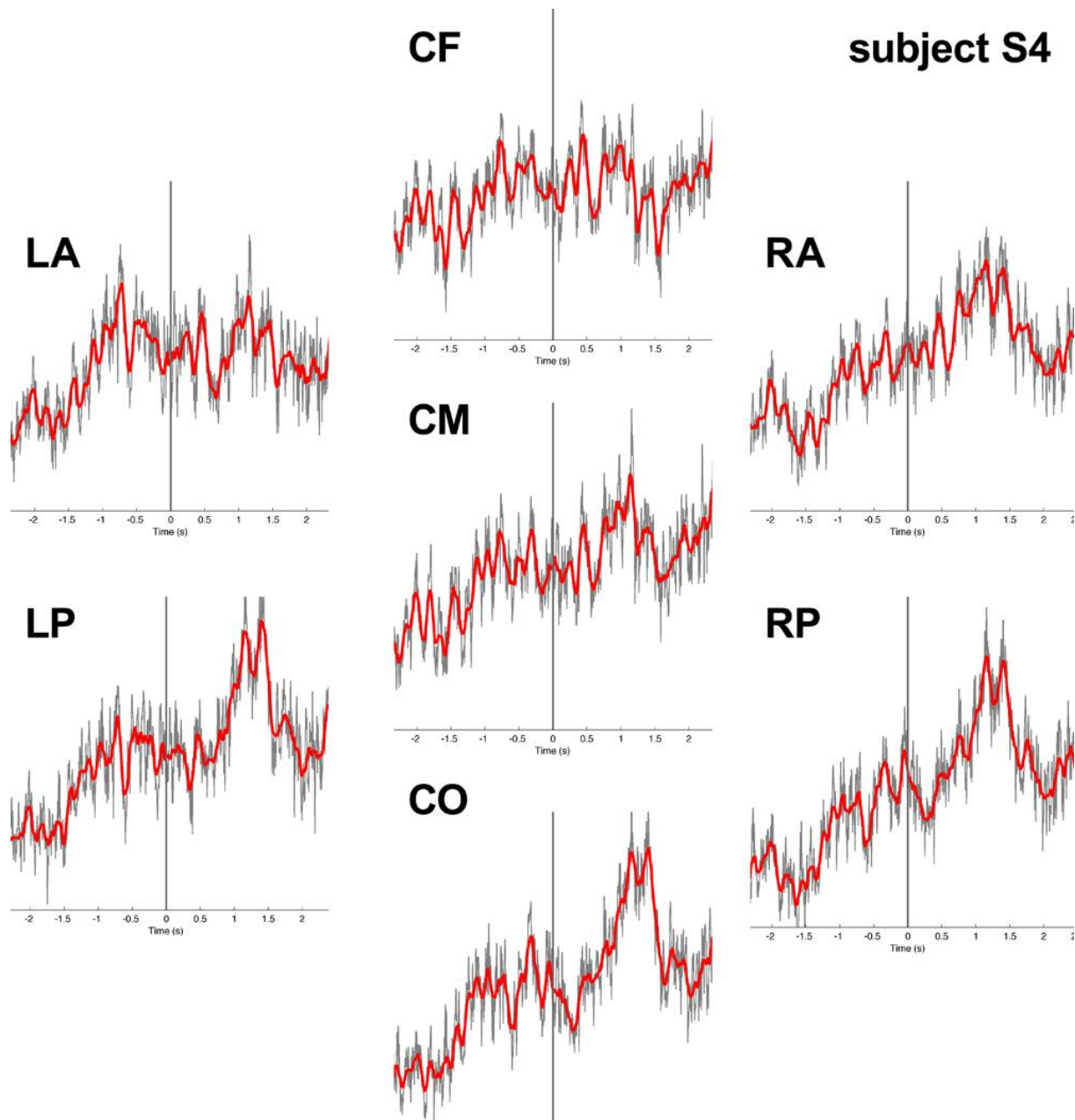


Figure 10. ERP plots for each ROI of subject S4, averaged across trials.

3.3. Fourier analysis

As only four subjects were measured and an average of 32 trials per subject were analyzed, it was first decided to pool all the data over the subjects and ROIs together on the single trial-level. To measure the difference between the conditions (N1 sleep and wake state), the frequencies were averaged in full frequency spectrum. The Jarque-Bera goodness-of-fit test of composite normality indicated that for the two conditions of the Fourier transform data the null hypothesis (“the data are normally distributed”) can be rejected at the 5% significance level. Thus, the Wilcoxon

matched-pairs signed-rank one-tailed test was used for determining difference between conditions ($p < 0.05$). The tests were one-tailed as we had a clear prediction: There is an increase in power across all frequencies during the transition from N1 sleep to wakefulness [30].

It was observed that the average DFT values were significantly lower in N1 condition ($p < 10^{-45}$). The average proportion of the awake state power spectrum to the N1 sleep power spectrum was found to be 1.07. The power spectrum for both conditions is illustrated in the Figure 11.

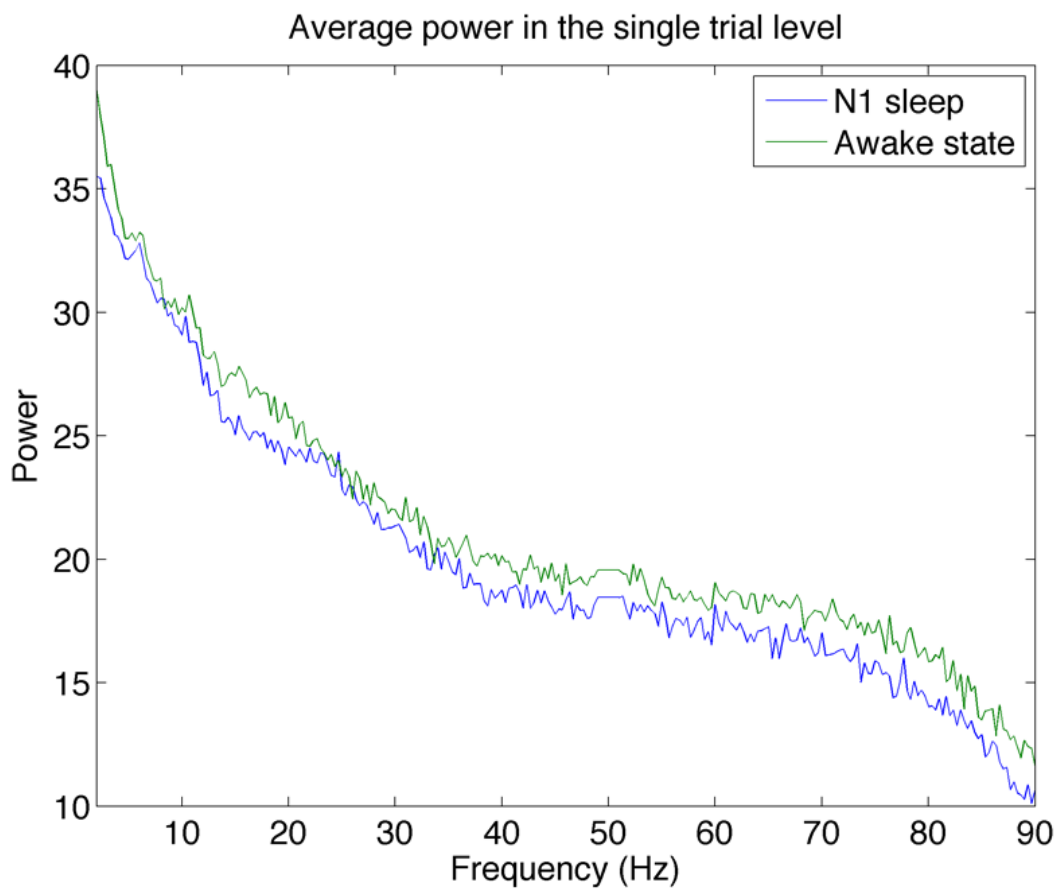


Figure 11. The averaged power spectrum across the subjects, trials, and ROIs for both N1 sleep and wake state.

These results where all the trials from all the subjects are pooled together could be biased by strong effects coming from one or two subjects. However, when analysed separately subject by subject, we can see that the average power was lower in all subjects for the sleep condition (See Figure 12). The Wilcoxon test revealed a significantly lower average power in the N1 condition for all the subjects (average $p < 10^{-10}$). The proportion of the awake state power spectrum to the N1 sleep power spectrum was found 1.10, 1.09, 1.03, 1.04 for each subject respectively.

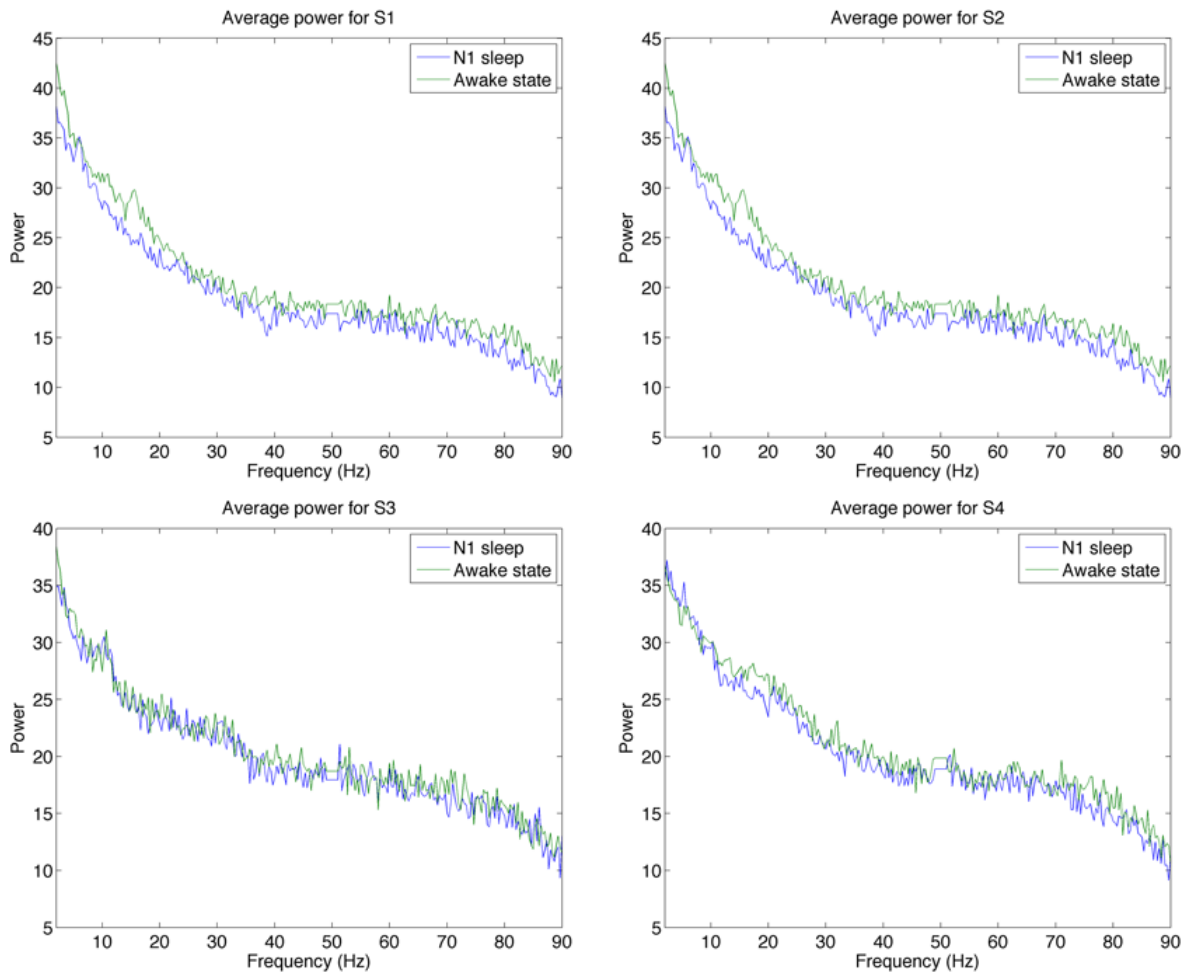


Figure 12. The power of the frequencies represented for each subject separately. The power spectrum (green) was found to be significantly higher for awake state compared to the sleep period (blue).

3.4. Time-frequency representation

The time-frequency analysis allowed to pool together all the trials of all subjects and see the change of spectral power over time on the group level (See Figure 13).

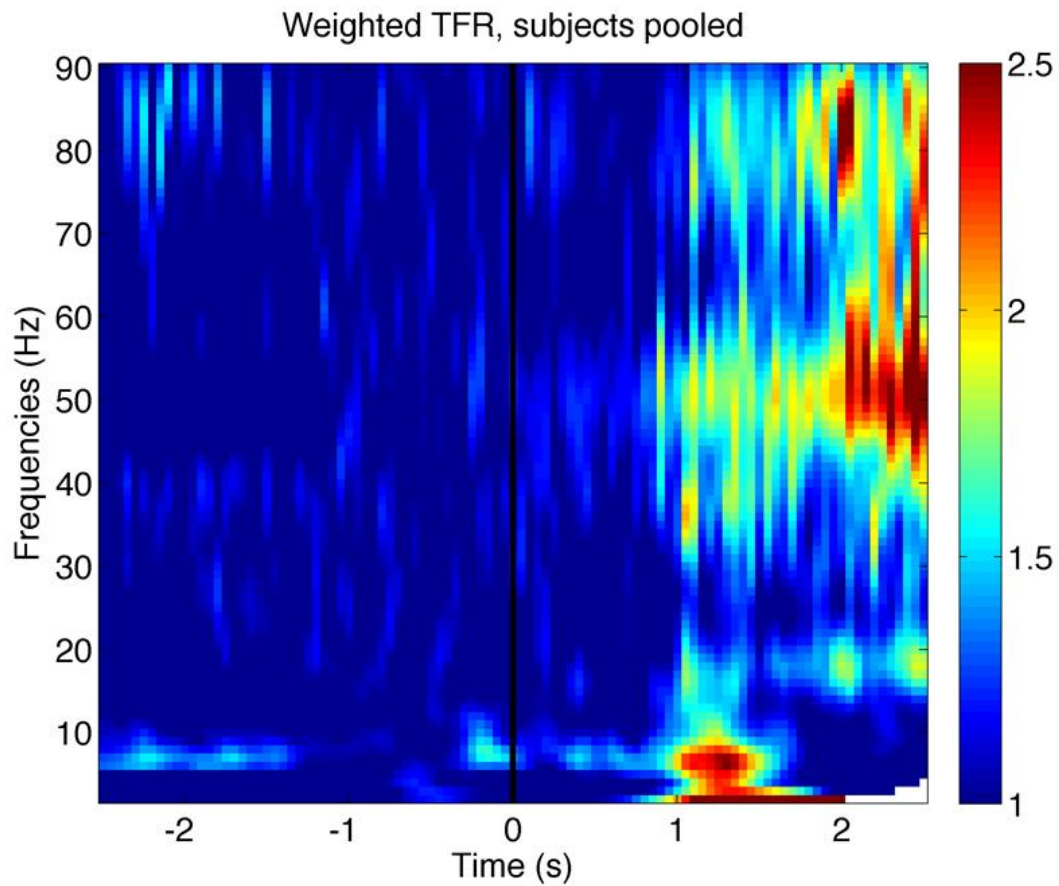


Figure 13. The transition from N1 to W led to the increase of power in the γ -band frequencies from 1 second after awakening. X-axis represents time (-2.5-2.5 s from awakening) and y-axis represents the full frequency range (2-90 Hz). The baseline (-400 to -100 ms) has been normalized to mean equal to 1.

To further analyze the EEG power spectrograms, the transition to W was observed in the ROI-level. We observed similar state-dependent patterns across the seven different forebrain areas (Figure 14).

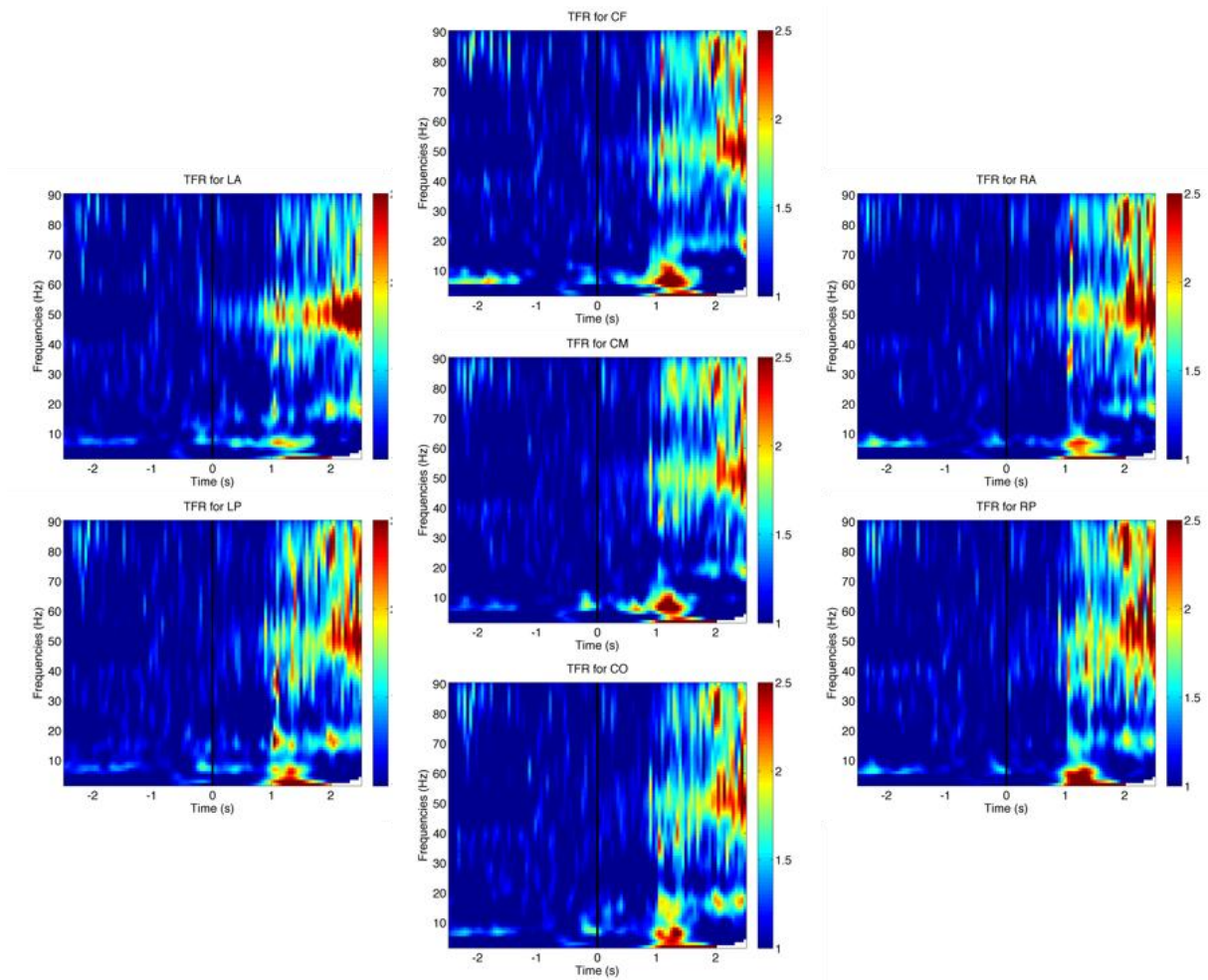


Figure 14. Spectrograms for the state transition in seven ROIs all subjects pooled. X-axis represents time (-2.5-2.5 s from awakening) and y-axis represents the full frequency range (2-90 Hz). The baseline (-400 to -100 ms relative to the awakening stimulus) was normalized to mean equal to 1.

The fact that these effects are temporally specific (to 1 second after awakening stimulus) across all ROIs shows that they are not arbitrary or artifactual effects of e.g. eye movement (which were at all removed in the pre-processing). Taken together, the awakening related spectral analysis shows a stronger spectral power emerging 1 second after awakening stimulus in the alpha and gamma bands (40-60 Hz and 70-90 Hz) relative to the baseline before awakening.

3.5. State space analysis

To characterize the dynamics of the phase transition happening at awakening, the variations in spectral patterns of EEG activity were analyzed. The conventionally scored N1 sleep, wake state and transition (1 second after awakening) consistently mapped to distinct regions of the state space (Figure 15). For the three subjects (except S3), the clusters were distinctive by eye from each other. As expected from the spectrograms, the transition clusters were largely overlapping with the N1 clusters.

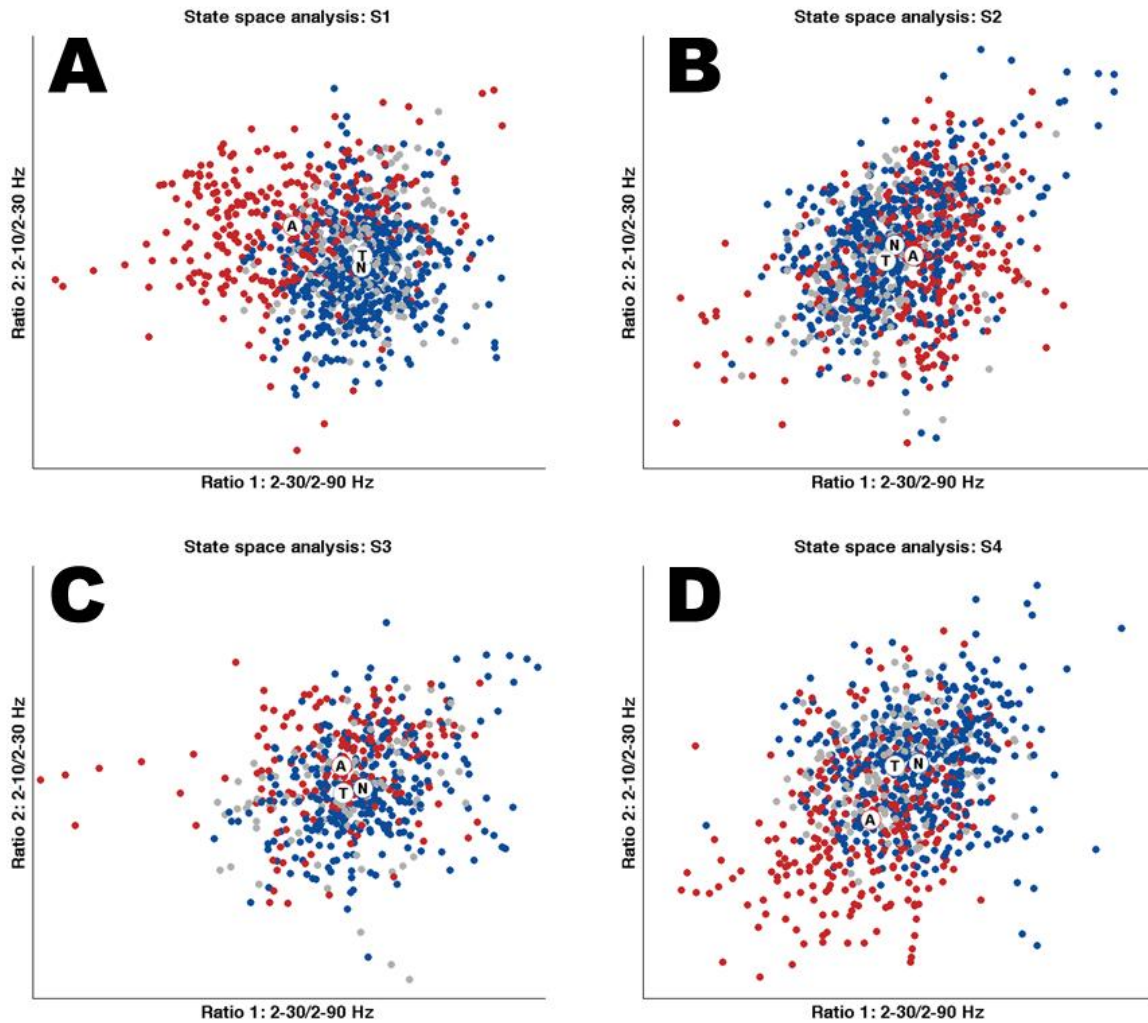


Figure 15. Spectral ratios of EEG activity define a two-dimensional state space. Each plot shows 6 seconds of EEG activity, and each point 0.5 second of EEG activity. In these graphs, the color of each state space point is determined from conventional scoring: N1 sleep (blue), Transition (grey), and wake state (red). Centroids of each cluster are denoted by white dots and corresponding letters A for Awake, T for Transition, and N for N1 sleep. **A.** State space analysis for subject S1. **B.** State space analysis for subject S2. **C.** State space analysis for subject S3. **D.** State space analysis for subject S4.

To quantify the difference between the three clusters, the Euclidean distance between the centre point pairs was calculated. The subjects could be grouped into two by the characteristics of distances. For subjects S1 and S4, the longest was the distance between the wake state and N1, and the closest between N1 and Transition period cluster centroids (Table 1). This reflects lower proportion of the non- γ bands in the wake state compared to N1 sleep and vice versa. For subjects S2 and S3 the most disjointed clusters were the wake state and Transition period. Surprisingly, for S2 the wake state and N1 were the closest, whereas for S3 the Transition and N1 sleep clusters were almost overlapping. The permutation test revealed significant ($p < 0.001$) distance between all the Awake and N1 sleep, and Awake and Transition clusters. The centroid distances did not differ significantly between the N1 and Transition clusters.

Table 1. Distances for the state space clusters for each subject. The function $d(State1, State2)$ illustrates Euclidean distance between mean values of the State1 and State2 cluster in the state space. For presentation clarity, the distances are multiplied by 100. The p-value is shown in brackets.

Subject (Nr of trials)	$d(Wake, N1)$	$d(Wake, Transition)$	$d(N1, Transition)$
S1 (35)	17.628 ($p < 0.0001$)	15.888 ($p < 0.0001$)	3.134 ($p < 0.0358$)
S2 (39)	4.659 ($p < 0.0001$)	5.679 ($p < 0.0003$)	4.817 ($p < 0.0014$)
S3 (21)	7.215 ($p < 0.0001$)	7.705 ($p < 0.0002$)	3.43 ($p < 0.0578$)
S4 (32)	17.492 ($p < 0.0001$)	15.536 ($p < 0.0001$)	3.909 ($p < 0.0194$)

4. Discussion

4.1. Main results

4.1.1. Event-related potentials

The aim of this thesis was to characterize the phase transition happening at awakening by numerical and computational methods. The author of the thesis covered all the steps from data acquisition to computer based signal processing (pre-processing algorithm) and analysis (e.g. ERPs, power spectrogram). To add, the dynamics of the sleep-wake transition were examined by a custom state mapping technique. Taken together, these observations provide empirical evidence that the electrophysiological processes at the moment of awakening are non-stationary.

In the first part of the analysis, the event-related potentials (ERPs) were computed to observe the change in the brain potentials after the awakening stimulus. We observed a strong amplitude shift starting at 1 second after the awakening stimulus. If the ERPs would have been demeaned to 0 relative to the baseline window, the potentials that go up after the awakening stimulus could be called “positive” and the potentials that go down “negative”. Thus, we can say that the shift in amplitude was towards positive potentials for subjects S1, S2, and S4, and negative potentials for subject S3 (See Figure 6).

In literature, this kind of slow (mainly $< 1\text{ Hz}$) fluctuation of amplitude in the EEG is called slow cortical potential (SCP). The SCP could be both a positive (potentials go up) or negative (potentials go down) shift in EEG amplitude relative to the baseline window. Previously, SCP negativity has been found to index increase in the excitability of the neurons in the superficial layers of the cerebral cortex and proposed to directly contribute to the emergence of consciousness (i.e. wakefulness) [31]. Besides numerous studies that show that SCP negativity is necessary for or accompanied with conscious experience (e.g. [32]), this conjecture has also been supported by findings from the Talis Bachmann laboratory in Tallinn ([33], [34]). Significantly, it has been hypothesized that whenever there is a change in the state of consciousness, there should be a change in the SCPs [31]. Visual observation of the ERPs computed in this thesis revealed SCPs for all of the subjects that could confirm to this hypothesis.

4.1.2. Power spectrum analysis

The results from the discrete Fourier transform indicated an overall increase in the amplitude of power spectrum linked to the awakening stimulus. Since the EEG was first described in the end

of 19th century, simple behaviours have been related to robust changes in the oscillatory activity, e.g. sleep onset increases θ -rhythms (4-7 Hz) [12]. However, on top of these oscillatory changes the existence of broadband changes across all frequencies during change in behaviour has been empirically proven, and a power-law process of the form $P(f) \sim A \cdot f^{-\chi}$ has been found [30]. The exponent χ in the power-law $P(f)$ for frequency f suggests a change in the correlation between neural populations, whereas the coefficient A suggests an overall change in population activity. Accordingly, the overall significant change seen in the power spectrum can be attributed to the change of the proportion coefficient $A_{all} = 1.07$, whereas within subjects change to the proportion coefficients $A_{S1} = 1.10, A_{S2} = 1.09, A_{S3} = 1.03, A_{S4} = 1.04$ for each subject respectively.

Interestingly, these shifts in the power of a broad range of frequencies have also been reported previously. In a study where data were gathered with intracranial (under the scalp directly on the cortex) recordings [35] Aru and colleagues observed a localized strong and sustained response in the power of a broad range of frequencies (50-150 Hz) – this could be seen as a local “awakening” where a cortical area gets activated by the visual stimulus. Indeed, it has been proposed that the sleep-wake transition is in many aspects similar to the local level processes in the brain, only that the sleep-wake transition happens globally [36]. This conjecture is supported by the “local sleep” phenomenon discovered in rats where some areas of the brain are locally asleep even during wakefulness [37]. Taken together, the sleep-wake transition could also be seen focally across the cerebral cortex.

4.1.3. Time-frequency representation

The group-level time-frequency representation of the data revealed two γ power bands in the ranges of 40-60 Hz and 70-90 Hz emerging gradually after the awakening stimulus. These γ -bands became prominent from roughly 1 second after awakening with a power of 1.5-2.5 times higher than the baseline. This relative increase in the power of the γ -bands is in accordance with the general notion that the activity of γ frequencies (30-90 Hz) is a signature of cortical activation [38]. For example, gamma power has been found to be stronger after caffeine administration [39].

The γ -bands seen in this study were also accompanied by α -rhythms with a power up to 2 times stronger than the baseline equivalent. The spectral increase in those bands across all ROIs suggests that these areas are synchronously modulated and all informative about the two states and the transition in between [9]. Nevertheless, the α -rhythms were most prominent in the

occipital lobe (CO) across subjects, typical for quiet wake state [12]. The γ power was strongest bilaterally in the frontal lobe (LA, RA), a region of the brain responsible for attention, executive functions, and speech.

4.1.4. State mapping

In the state space analysis of the EEG, the N1 sleep and wake state were consistently identified as significantly distinct spectral clusters (See Table 1). The difference between the Transition and N1 cluster centroids was ambiguous and insignificant, though there were near significant differences in the centroid locations. This, however, supports the hypothesis that the awakening takes about 1 second from the awakening stimulus. The significance of the distance of the N1 and W cluster centroids supports the notion that the two major behavioural states are represented by different dynamics of neural processing. In this sense, the extreme regions of the N1 and W clusters in the Ratio 1 axis correspond to γ -rich wakefulness and γ -poor N1 sleep respectively. Despite of lack of consistency in the specificity of the Ratio 2 across subjects, the state space indicates a slight difference in the proportion of below 10 Hz brain rhythms for the N1 and W within subjects, as predicted.

Although the state space techniques have been applied to EEG recordings in rodents before (e.g. [1], [9]), this thesis has shown that the method can successfully be used to detect the sleep-wake transitions in humans. The state space analysis does not assume averaging across trials or subjects, allowing behavioural changes to be detected without many observations. In another words, the state space technique could be used in machine learning to classify mental states. This could be useful in many practical applications that use EEG to detect sleep-wake transitions.

Perhaps the most interesting result of this study is that the transition from N1 sleep to wakefulness in humans takes about 1 second. We explored the ERPs, TFR, power spectrogram, and the state space which all indicated a palpable change in the EEG 1 second after the awakening stimulus. The previous studies have shown that the transition from SWS to wakefulness takes 1 second in rodents [3]. Based on the empirical findings of this study, it is also reasonable estimate for the sleep-wake transition in humans.

4.2. Methodological considerations

First, the most important requirement for computing ERPs (i.e. averaging over trials) is that the signal added to the averaging must be aligned at the exact moment of awakening [19]. This requirement was not fulfilled as the loose note down of the awakening stimulus had a precision

of 0.5 seconds. This methodological shortage did not allow for meaningful short-latency ERP analysis. Fortunately, this was compensated by the long-latency ERP analysis. Second, in the previous studies with rodents (e.g. [1], [9]) the state space analysis has been used with data recorded during much longer time period (24, 48, and 72 hours) than these data. In this thesis, the abrupt transition to wake state was captured with the state space technique, but a longer recording is needed to detect behavioural characteristics marking e.g. drowsiness. Last, the small sample size of only 4 subjects makes this study as very preliminary and further studies should confirm the results.

4.3. Future work

Hopefully this thesis contributes to solving some questions about sleep-wake transitions in the future. Future studies could be devoted to reveal if speed of transition is related to the state before, and whether phase transition could be characterized by the trajectory of the consecutive sequences of points in the state space. The state space technique developed for humans could also be used to determine the difference between healthy subjects and patients with neurological deficiencies. Most importantly, the characteristics of the sleep-wake transition explored in this thesis could be used in everyday applications that use EEG to measure brain activity, future sleep research, and medicine to detect rapid sleep-wake transitions in humans.

Future studies could also use longer recordings that allow for the use of elegant computational analysis methods. For example, a generalization of the wavelet transform called matching pursuit could be used to determine more complex and rapidly varying characteristics of the patterns embedded in sleep-wake transitions. This method could reveal characterizing transients appearing randomly in the signal that are not easily detectable by Fourier or wavelet basis.

Last, further work could to be done to reveal in which ROI(s) the SCPs were the strongest. It could also be found whether the amplitude shift seen 1 second after the awakening stimulus could differ bilaterally or between the frontal and occipital areas. For example, previous work of Stamm et. al. [33] suggests that the central-right areas of the cortex are more strongly involved in the SCP effect.

Conclusions

To summarize, all the steps of processing and analysis applied for biological time series, such as human EEG data, were done in this thesis. More technically, modern computational methods were used to characterize the phase transition happening at awakening. These data revealed an amplitude fluctuation in the event-related-potentials, a significant increase in the power of a broad range of frequencies attributed to the proportion coefficient A , a salient emergence of γ and α power 1.5-2.5 times higher compared to the baseline, and a geometrical transpose in the state space all roughly 1 second after the awakening stimulus. These observations support the prediction that the transition from sleep to wake state takes 1 second in humans. This study provides measures to quantify the abrupt state switch in humans and hopefully helps to resolve some questions regarding the sleep-wake transition.

References

- [1] D. Gervasoni, S.-C. Lin, S. Ribeiro, E. S. Soares, J. Pantoja, and M. A. L. Nicolelis, "Global Forebrain Dynamics Predict Rat Behavioral States and Their Transitions," *J. Neurosci.*, vol. 24, no. 49, pp. 11137–11147, Dec. 2004.
- [2] American Academy of Sleep Medicine, "Drowsy Driving Fact Sheet," 2009. [Online]. Available: <http://www.aasmnet.org/Resources/FactSheets/DrowsyDriving.pdf>. [Accessed: 13-May-2014].
- [3] C. B. Saper, P. M. Fuller, N. P. Pedersen, J. Lu, and T. E. Scammell, "Sleep State Switching," *Neuron*, vol. 68, no. 6, pp. 1023–1042, Dec. 2010.
- [4] D. T. J. Liley and I. Bojak, "Understanding the Transition to Seizure by Modeling the Epil... : Journal of Clinical Neurophysiology," *J. Clin. Neurophysiol.*, vol. 22, no. 5, pp. 300–313, 2005.
- [5] B. D. Fulcher, A. J. K. Phillips, and P. A. Robinson, "Modeling the impact of impulsive stimuli on sleep-wake dynamics," *Phys. Rev. E*, vol. 78, no. 5, p. 051920, Nov. 2008.
- [6] A. J. K. Phillips, P. A. Robinson, D. J. Kedziora, and R. G. Abeysuriya, "Mammalian Sleep Dynamics: How Diverse Features Arise from a Common Physiological Framework," *PLoS Comput Biol*, vol. 6, no. 6, p. e1000826, Jun. 2010.
- [7] M. J. Rempe, J. Best, and D. Terman, "A mathematical model of the sleep/wake cycle," *J. Math. Biol.*, vol. 60, no. 5, pp. 615–644, May 2010.
- [8] E. Hwang, S. Kim, K. Han, and J. H. Choi, "Characterization of Phase Transition in the Thalamocortical System during Anesthesia-Induced Loss of Consciousness," *PLoS ONE*, vol. 7, no. 12, p. e50580, Dec. 2012.
- [9] C. G. Diniz Behn, E. B. Klerman, T. Mochizuki, S.-C. Lin, and T. E. Scammell, "Abnormal Sleep/Wake Dynamics in Orexin Knockout Mice," *Sleep*, vol. 33, no. 3, pp. 297–306, Mar. 2010.
- [10] G. Pocock and C. D. Richards, *The human body: an introduction for the biomedical and health sciences*. Oxford University Press, 2009.
- [11] M. Gazzaniga, R. B. Ivry, and G. R. Mangun, *Cognitive Neuroscience: The Biology of the Mind*, Fourth Edition edition. New York, N.Y: W. W. Norton & Company, 2013.
- [12] R. A. Shatzmiller and A. A. Gonzalez, "Sleep Stage Scoring," 2010.
- [13] K. Takahashi, J.-S. Lin, and K. Sakai, "Characterization and mapping of sleep-waking specific neurons in the basal forebrain and preoptic hypothalamus in mice," *Neuroscience*, vol. 161, no. 1, pp. 269–292, Jun. 2009.
- [14] "MATLAB homepage," 2014. [Online]. Available: <http://www.mathworks.se/products/matlab/>.
- [15] R. Oostenveld, P. Fries, E. Maris, and J.-M. Schoffelen, "FieldTrip: Open Source Software for Advanced Analysis of MEG, EEG, and Invasive Electrophysiological Data," *Comput. Intell. Neurosci.*, vol. 2011, Dec. 2010.
- [16] R. Oostenveld, "FieldTrip homepage," 2013. [Online]. Available: <http://fieldtrip.fcdonders.nl/start>. [Accessed: 22-Apr-2014].
- [17] "Reference: ft_preprocessing," 2013. [Online]. Available: http://fieldtrip.fcdonders.nl/reference/ft_preprocessing. [Accessed: 22-Apr-2014].
- [18] "Reference: appenddata," 2013. [Online]. Available: <http://fieldtrip.fcdonders.nl/reference/appenddata>. [Accessed: 22-Apr-2014].
- [19] R. M. Rangayyan, *Biomedical Signal Analysis: A Case-Study Approach*, 1 edition. Piscataway, NJ : New York, N.Y: Wiley-IEEE Press, 2001.

- [20] H. Aurlien, I. O. Gjerde, J. H. Aarseth, G. Eldøen, B. Karlsen, H. Skeidsvoll, and N. E. Gilhus, "EEG background activity described by a large computerized database," *Clin. Neurophysiol.*, vol. 115, no. 3, pp. 665–673, Mar. 2004.
- [21] "Matlab Documentation Center: ksdensity," *ksdensity - Kernel smoothing function estimate*, 2014. [Online]. Available: <http://www.mathworks.se/help/stats/ksdensity.html>. [Accessed: 22-Apr-2014].
- [22] "Reference: ft_channelrepair," 2013. [Online]. Available: http://fieldtrip.fcdonders.nl/reference/ft_channelrepair. [Accessed: 23-Apr-2014].
- [23] "Reference: ft_rejectvisual," 2013. [Online]. Available: http://fieldtrip.fcdonders.nl/reference/ft_rejectvisual. [Accessed: 23-Apr-2014].
- [24] S. Roberts and R. Everson, Eds., *Independent component analysis: principles and practice*. Cambridge: Cambridge University Press, 2001.
- [25] "Use independent component analysis (ICA) to remove EOG artifacts," 2014. [Online]. Available: http://fieldtrip.fcdonders.nl/example/use_independent_component_analysis_ica_to_remove_eog_artifacts. [Accessed: 23-Apr-2014].
- [26] P. Bloomfield, *Fourier Analysis of Time Series: An Introduction*. Wiley, 1976.
- [27] Ü. Lepik and H. Hein, *Haar Wavelets: With Applications*, 2014 edition. Cham ; New York: Springer, 2014.
- [28] "Reference: ft_freqanalysis," 2013. [Online]. Available: http://fieldtrip.fcdonders.nl/reference/ft_freqanalysis. [Accessed: 28-Apr-2014].
- [29] "Savitzky–Golay filter," *Wikipedia, the free encyclopedia*, 2014. [Online]. Available: http://en.wikipedia.org/w/index.php?title=Savitzky%E2%80%93Golay_filter&oldid=605218796. [Accessed: 28-Apr-2014].
- [30] K. J. Miller, L. B. Sorensen, J. G. Ojemann, and M. den Nijs, "Power-Law Scaling in the Brain Surface Electric Potential," *PLoS Comput Biol*, vol. 5, no. 12, p. e1000609, Dec. 2009.
- [31] B. J. He and M. E. Raichle, "The fMRI signal, slow cortical potential and consciousness," *Trends Cogn. Sci.*, vol. 13, no. 7, pp. 302–309, Jul. 2009.
- [32] D. Pins and D. Ffytche, "The Neural Correlates of Conscious Vision," *Cereb. Cortex*, vol. 13, no. 5, pp. 461–474, May 2003.
- [33] M. Stamm, J. Aru, and T. Bachmann, "Right-frontal slow negative potentials evoked by occipital TMS are reduced in NREM sleep," *Neurosci. Lett.*, vol. 493, no. 3, pp. 116–121, Apr. 2011.
- [34] C. Murd, J. Aru, M. Hiio, I. Luiga, and T. Bachmann, "Caffeine enhances frontal relative negativity of slow brain potentials in a task-free experimental setup," *Brain Res. Bull.*, vol. 82, no. 1–2, pp. 39–45, Apr. 2010.
- [35] J. Aru, N. Axmacher, A. T. A. D. Lam, J. Fell, C. E. Elger, W. Singer, and L. Melloni, "Local Category-Specific Gamma Band Responses in the Visual Cortex Do Not Reflect Conscious Perception," *J. Neurosci.*, vol. 32, no. 43, pp. 14909–14914, Oct. 2012.
- [36] K. D. Harris and A. Thiele, "Cortical State and Attention," *Nat. Rev. Neurosci.*, vol. 12, no. 9, pp. 509–523, Aug. 2011.
- [37] V. V. Vyazovskiy, U. Olcese, E. C. Hanlon, Y. Nir, C. Cirelli, and G. Tononi, "Local sleep in awake rats," *Nature*, vol. 472, no. 7344, pp. 443–447, Apr. 2011.
- [38] M. H. J. Munk, P. R. Roelfsema, P. König, A. K. Engel, and W. Singer, "Role of Reticular Activation in the Modulation of Intracortical Synchronization," *Science*, vol. 272, no. 5259, pp. 271–274, Apr. 1996.

- [39] J. Aru, K. Korjus, C. Murd, and T. Bachmann, "Spectral Signatures of the Effects of Caffeine and Occipitally Applied Transcranial Magnetic Stimulation in a Task-Free Experimental Setup," *J. Caffeine Res.*, vol. 2, no. 1, pp. 23–30, Mar. 2012.

Appendix

I MATLAB code

The MATLAB scripts written for the pre-processing and analysis done in this thesis are included as on-line supplementary material with this thesis.

II Licence

Non-exclusive licence to reproduce thesis and make thesis public

I, **Kristjan-Julius Laak** (date of birth: 03.12.1991), herewith grant the University of Tartu a free permit (non-exclusive licence) to:

- 1.1. reproduce, for the purpose of preservation and making available to the public, including for addition to the DSpace digital archives until expiry of the term of validity of the copyright, and
- 1.2. make available to the public via the web environment of the University of Tartu, including via the DSpace digital archives until expiry of the term of validity of the copyright,

Investigating the phase transition in human brain at the moment of awakening,

supervised by Raul Vicente and Jaan Aru,

2. I am aware of the fact that the author retains these rights.
3. I certify that granting the non-exclusive licence does not infringe the intellectual property rights or rights arising from the Personal Data Protection Act.

Tartu, **14.05.2014**